OPTICS STUDIES FOR THE INTERACTION REGION OF THE INTERNATIONAL LINEAR COLLIDER

R.Versteegen#, O. Delferrière, O. Napoly, J. Payet, D. Uriot
CEA, Irfu/SACM, Gif-sur-Yvette, France

Abstract

Simulations of beam transport in the Interaction Region (IR) of the International Linear Collider (ILC) for both L*=3.5m and L*=4.5m (final drift length) are presented. Solenoid and anti-'Detector Integrated Dipole' (anti-DID) effects are considered, including the influence of Synchrotron Radiation (SR), as well as distortions arising from the insertion of a crab cavity.

INTRODUCTION

In the International Linear Collider (ILC) reference design [1] nominal beam sizes at the Interaction Point (IP) are $\sigma_{x0} = 640$nm and $\sigma_{y0} = 5.7$nm. This strong focusing enables the nominal luminosity $L_0 = 2.10^{34}$cm^{-2}.s^{-1} to be reached. Two IR in a push-pull configuration are considered, one will have L*=3.5m and use the Silicon Detector (SiD) concept, the second one will have L*=4.5m and use the International Large Detector (ILD) concept. Both are based on a collision with 14mrad total crossing angle, implying that the detector solenoid axis and the machine axis do not coincide. This provokes severe effects on the beam size and trajectory which have to be compensated to restore the nominal luminosity [2]. The orbit deviation in the IR induces SR which is a new cause of beam size growth, but cannot be compensated. Anti-DID is considered to reduce background in the detector [3]. It creates vertical dispersion in the IR and doubles crossing angle effects on the incoming beam. Only the vertical plane is considered here, assuming that effects in the horizontal plane are negligible.

Correction of detector solenoid and anti-DID effects are presented in the first part of this paper. Then simulation results including SR are exposed. Finally the insertion of the crab cavity is considered. Particles receive horizontal kicks in the crab cavity to compensate the luminosity loss due to the crossing angle. In the presence of the solenoid, it induces a vertical crab crossing to be compensated not to lose luminosity.

COMPENSATION OF SOLENOID AND ANTI-DID EFFECTS

Solenoid and anti-DID effects

The introduction of the solenoid has two major effects:

- the longitudinal field introduces coupling between horizontal and vertical motions, resulting in beam size growth,
- particles penetrate the solenoid field off axis because of the crossing angle. The central trajectory is deviated, and vertical dispersion is generated.

#reine.versteegen@cea.fr

In addition, the detector solenoid fringe field is overlapping with final focus elements, essentially with the last quadrupole QD0 as shown in Figure 1. Coupling is modified and natural compensation between longitudinal and radial fields of solenoid is broken, leading to non-zero orbit at the IP, as illustrated in Figure 2.

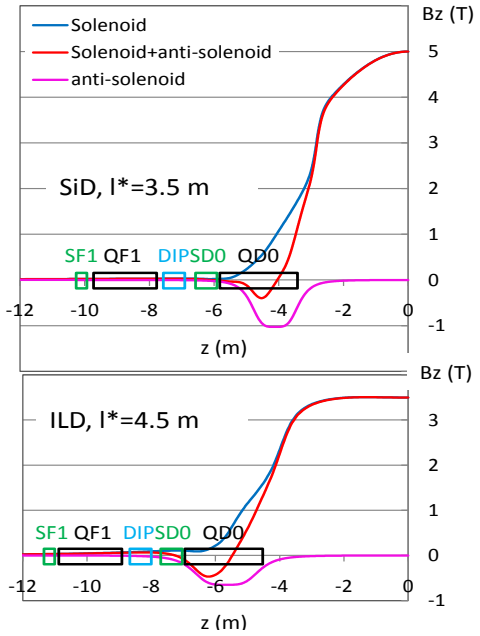

Figure 1: Longitudinal field component for both detector solenoids. An optimized anti-solenoid field is represented and final focus system elements are positioned. DIP is an additional dipole corrector. IP is at z=0.

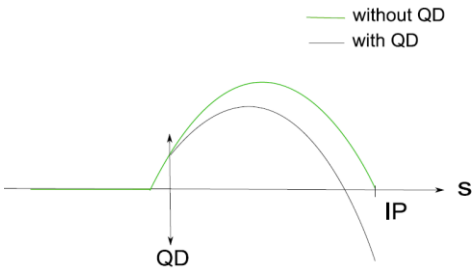

Figure 2: Schematic of vertical orbit deviation in solenoid field overlapping with the final focusing quadrupole QD.

Inserting the anti-DID consists in adding a horizontal field component, so that pairs created during collisions are directed towards the extraction line. Consequently the incoming beam sees double crossing angle from the orbit point of vue, and vertical dispersion rises.

Table 1 summarizes results of simulations for L*=3.5m and L*=4.5m and corresponding detector solenoid field. One can see that effects of ILD solenoid are more important compared to SiD in case of L*=3.5m, even if peak field of ILD solenoid is smaller. This is due to the integration of overlapping effects of solenoid with QD0 from the final focusing quadrupole to the IP [2].

Table 1: Solenoid and anti-DID effects on vertical beam size and orbit at the IP.

	SiD, L*=3.5 m		**ILD, L*=4.5 m**	
	$\mathbf{y_{IP}}$	$\boldsymbol{\sigma_y/\sigma_{y0}}$	$\mathbf{y_{IP}}$	$\boldsymbol{\sigma_y/\sigma_{y0}}$
Solenoid	-12.6 μm	23	-25 μm	49
Solenoid +anti-DID	-150 μm	27	-323.9 μm	57.4

Correction of the beam orbit and size at the IP

The main corrector acting on coupling and trajectory is the weak anti-solenoid [2]. It has three parameters to be optimized: length, peak field and position. In this purpose an optimization code has been developed and DIMAD [4] was used for simulations. Solenoid field map is described using solenoid slices, and thin lenses are inserted in between to introduce final focus system elements in the field. The anti-solenoid field is added to the main solenoid field in the field map. Crossing angle is represented using displacements of the reference trajectory. At each iteration, a file describing the IR is generated and DIMAD is automatically run. Figure 1 shows the modified longitudinal field for both detector cases after optimization of the length, the peak field and the position of the anti-solenoid (red curves).

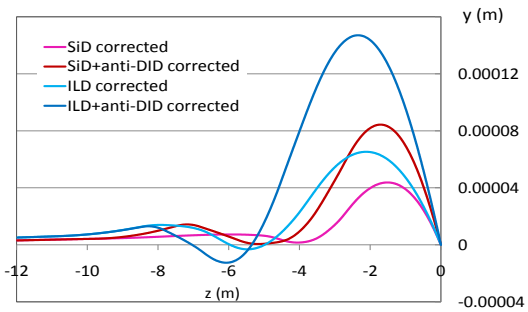

Figure 3: Compensated vertical central trajectories for both detector solenoids. IP is at z=0.

Full compensation of solenoid effects is obtained using additional correctors and tuning knobs. This, as well as the addition of the anti-DID, is done using TraceWin tracking code [5]. TraceWin enables easier treatment of superimposed magnetic field maps. The anti-DID is added as a field map, so that vertical dispersion is correctly generated and taken into account. Vertical central trajectories after total correction are plotted in Figure 3.

The optimization of the anti-solenoid is different depending on the detector solenoid (and L*). In case of SiD solenoid, total correction with tuning knobs is quite easy. The anti-solenoid was optimized to compensate vertical orbit at the IP, then skew correction section and vertical displacements of sextupoles were tuned to restore the nominal beam size. Correction of anti-DID effects is independent. It uses three dipole correctors: two superimposed with final doublet, over QF1 and QD0; and one additional dipole corrector 'DIP' located between QF1 and SD0 (Figure 1). If same criteria are chosen in case of ILD solenoid for the anti-solenoid optimization, we obtain $\sigma_y/\sigma_{y0} \sim 6.1$. This is too high to be corrected with tuning knobs. For this reason, the anti-solenoid was optimized to reduce the beam size and the additional dipole corrector DIP was used to restore zero orbit. Tuning knobs are same as before, but horizontal displacements of sextupoles are needed as well. All three dipole corrector fields and the anti-solenoid peak field have to be re-tuned when the anti-DID is switched on. For all cases $\sigma_y/\sigma_{y0} = 1.005$ is reached after correction.

SYNCHROTRON RADIATION IN THE IR

Due to the strong focusing, SR is emitted in final doublet (Oide effect [6]), leading to beam size growth. Results taking SR into account in TraceWin simulations are given in Table 2.

Table 2: Beam size growth due to SR in the IR

	$\boldsymbol{\sigma_y/\sigma_{y0}}$
No Solenoid, L*=3.5m	1.001
SiD Solenoid	1.023
SiD Solenoid + anti-DID	1.027
No Solenoid, L*=4.5m	1.010
ILD Solenoid	1.030
ILD Solenoid + anti-DID	1.033

The effect of SR on beam size is negligible for L*=3.5m nominal lattice, whereas σ_y/σ_{y0}=1.0% for L*=4.5m lattice. Addition of the solenoid and the anti-DID inducing orbit deviation in final focus leads to maximum 3.3% beam size growth (ILD/L*=4.5m).

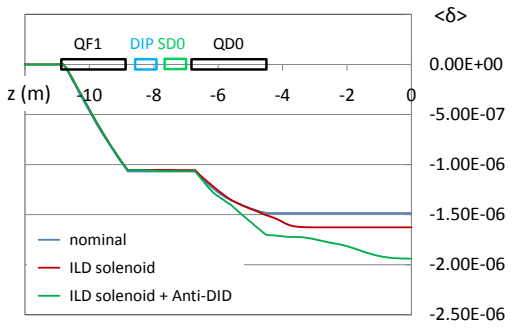

Figure 4: Evolution of average momentum in the IR for L*=4.5m. IP is at z=0.

SR induces an increase of momentum spread in the beam, and a diminution of the average energy along the IR. The average momentum evolution in the IR is plotted in Figure 4 in the case of L*=4.5m.

Variations of the momentum spread are small and very similar for the three studied cases (no solenoid, solenoid, solenoid + anti-DID). A difference can be noticed for the average momentum depending on the field in the IR. If the observed beam size growth given in Table 2 were due to energy loss in the IR, it could be compensated by retuning focusing quadrupoles. As it cannot, this means that beam size growth results essentially from the vertical dispersion, which depends on orbit deviation in the IR (Figure 3), and cannot be corrected.

INSERTION OF THE CRAB CAVITY

The crab cavity is inserted to give a transverse kick to particles depending on their longitudinal position in the bunch. It creates a progressive rotation of the beam to restore head on collision [7].

We assume that transverse potential in the cavity can be written as:

$$V_\perp = \mathrm{V}_{\perp 0} \sin\frac{2\pi f z}{c} \approx \mathrm{V}_{\perp 0}\frac{2\pi f}{c} z \qquad (1)$$

with $\mathrm{V}_{\perp 0} = \sqrt{V_{x0}^2 + V_{y0}^2}$ the amplitude, f the frequency, c the velocity of light and z the longitudinal coordinate within the bunch. The crab cavity can be modelled as a matrix MC introducing the $\langle x\ z\rangle$ correlation. The matrix will differ from Identity matrix by two terms (E_0 being the nominal energy in electronVolt):

$$MC25 = \frac{V_{x0}}{E_0}\frac{2\pi f}{c};\ MC45 = \frac{V_{y0}}{E_0}\frac{2\pi f}{c} \qquad (2)$$

The crab cavity matrix is inserted 13.4m from the IP. If R designates the transfer matrix from the crab cavity to the IP, modification of the coordinates at the IP are:

$$\begin{cases} \Delta x_{IP}(z) = (R12\ MC25 + R14\ MC45)z \\ \Delta y_{IP}(z) = (R32\ MC25 + R34\ MC45)z \end{cases} \qquad (3)$$

To restore head on collision $\Delta x_{IP}(z) \approx -z\ \theta_c$ is needed (θ_c being half crossing angle), and $\Delta y_{\mathrm{IP}} = 0$ for each z. According to (3), it leads to:

$$\begin{cases} MC25 = -\dfrac{R34}{R12\ R34 - R14\ R32}\theta_c \\ MC45 = -MC25\ \dfrac{R32}{R34} \end{cases} \qquad (4)$$

These expressions show that in case of nominal lattice without coupling, $R32$ will be zero and only a kick in the horizontal plane is needed. But when solenoid field is switched on, the additional term $MC45$ will be necessary to compensate for coupling from the crab cavity location to the IP. If coupling is not compensated ($MC45 = 0$), and for θ_c = 7mrad, the resulting vertical crab crossing angle θ_{cy} is given by:

$$\theta_{cy} = -\frac{R32\ R34}{R12\ R34 - R14\ R32}\theta_c \sim -60\mu rad \qquad (5)$$

θ_{cy} results from the horizontal crab crossing being transferred in the vertical plane. It leads to same amount of luminosity loss as if there was no cavity: $L \approx 0.3 * L_0$ (luminosity calculation with crossing angle [8]).

Using (2) and (4), values of cavity voltages for f=3.9GHz are calculated and given in Table 3.

Table 3: Crab cavity transverse voltages when detector solenoid is switched on.

	V_{x0}(MV)	V_{y0}(kV)
SiD Solenoid, L*=3.5 m	1.31	75.1
ILD Solenoid, L*=4.5 m	1.21	63.1

Taking crab crossing into account gives rise to distortions in the beam since particles are going off axis through the elements of the final focus system. But the vertical beam size growth due to these distortions has been found to be less than 1%, in case of fully compensated solenoid. Both SiD/L*=3.5m and ILD/L*=4.5m give similar results.

CONCLUSION

It has been shown in this paper that effects of the solenoid and the anti-DID can be corrected for SiD and ILD detectors. Synchrotron radiation in the interaction region cannot be compensated and leads to 3.3% beam size growth in the worst case. Coupling subsists in the lattice from the crab cavity location to the IP. It implies that horizontal kicks given in crab cavity are transferred in the vertical plane. It generates a vertical crab crossing at the IP, unless it is compensated. This can be done with a vertical component of the field in the crab cavity.

ACKNOWLEDGEMENTS

The authors would like to thank Mrs. D. Angal-Kalinin for her very helpful discussion and for providing ILC decks used for this work.

REFERENCES

[1] ILC Reference Design Report, 2007.
[2] Y. Nosochkov, A. Seryi, Phys. Rev. Let., 8, 021001, 2005.
[3] A. Seryi, *et al.*, SLAC-PUB-11662, 2006.
[4] R. Servranckz, *et al.*, SLAC-285, 1985.
[5] D. Uriot, TraceWIN code, http://irfu.cea.fr/Sacm/logiciels/index3.php.
[6] K. Oide, Phys. Rev. Let., Vol. 61, Nb. 15, 1988.
[7] R. Palmer, SLAC-PUB-4707, 1988.
[8] O. Napoly, CERN-SL 92-34 (AP), 1992.